Review of terahertz semiconductor sources*

Feng Wei(冯伟)†

Department of Physics, Jiangsu University, Zhenjiang 212013, China

Abstract: Terahertz (THz) technology can be used in information science, biology, medicine, astronomy, and environmental science. THz sources are the key devices in THz applications. The author gives a brief review of THz semiconductor sources, such as $GaAs_{1-x}N_x$ Gunn-like diodes, quantum wells (QWs) negative-effective-mass (NEM) THz oscillators, and the THz quantum cascade lasers (QCLs). THz current self-oscillation in doped $GaAs_{1-x}N_x$ diodes driven by a DC electric field was investigated. The current self-oscillation is associated with the negative differential velocity effect in the highly nonparabolic conduction band of this unique material system. The current self-oscillations and spatiotemporal current patterns in QW NEM p^+pp^+ diodes was studied by considering scattering contributions from impurities, acoustic phonons, and optic phonons. It is indicated that both the applied bias and the doping concentration strongly influence the patterns and self-oscillating frequencies. The NEM p^+pp^+ diode may be used as an electrically tunable THz source. Meanwhile, by using the Monte Carlo method, the device parameters of resonant-phonon THz QCLs were optimized. The results show that the calculated gain is more sensitive to the injection barrier width, the doping concentration, and the phonon extraction level separation, which is consistent with the experiments.

Key words: THz semiconductor sources; $GaAs_{1-x}N_x$ Gunn-like diode; negative-effective-mass THz oscillator; THz quantum cascade laser

DOI: 10.1088/1674-4926/33/3/031001 **PACC:** 7200; 7220H

1. Introduction

The terahertz (THz) frequency band is very promising in the applications of stratospheric astronomy, medical imaging technology, and large capacity mobile communication. Much effort has recently been devoted to the studies of THz generation by $GaAs_{1-x}N_x$ Gunn-like diodes, quantum wells (QWs) negative-effective-mass (NEM) THz oscillators, and THz quantum cascade lasers (QCLs).

The dilute nitride $GaAs_{1-x}N_x$ has become a unique system in semiconductor physics because of a number of qualitatively new alloy phenomena and electronic properties caused by the incorporation of N in GaAs[1, 2]. For example, it is well known that the band gap is strongly reduced. Additionally, the admixing of the N-impurity levels with the extended conduction-band states of GaAs makes the conduction band split into two highly nonparabolic bands, which is of interest for long-wavelength optoelectronic applications. It is demonstrated that this unusual band dispersion can be exploited to control the dynamics of conduction electrons. A strong negative differential velocity (NDV) effect in $GaAs_{1-x}N_x$ is observed when electrons are accelerated by an applied dc electric field into the NEM region of the subband[3]. The NEM dispersion can especially result in some interesting phenomena, such as current self-oscillation and complex nonlinear dynamics in different kinds of semiconductor systems[4−6].

The experiments in Refs. [7, 8] show that the dispersion relation for the ground subband of a p-type quantum well (QW) of zinc-blende-like semiconductors contains an extensive section with an NEM due to the spin-orbit coupling of heavy- and light-hole states and the symmetry breaking of the QW potential. By abstracting an analytical NEM dispersion relation from a p-type QW subband, several model calculations of carrier transport in p^+pp^+ diodes with a NEM p-base have been performed, by using the collisionless Boltzmann equation and the nonparabolic balance-equation theory[9]. The calculations in Ref. [5] indicated that the steady-state velocity-field curve of carriers with an NEM dispersion supports a N-shaped negative differential velocity (NDV) section, which can lead to the formation of electric-field domains and self-oscillating currents. The frequency may be controlled by varying the QW widths and the doping concentration in QWs. The self-oscillating frequency lies in the THz range for EM p^+pp^+ diodes having submicrometer p-base lengths.

The typical and the most successful demonstration of intersubband transition design is the quantum-cascade laser (QCL). The key feature of QCLs is that the active region consists of dozens or hundreds of cascaded modules. Though QCLs are very successful in the mid-infrared range, it is not easy to fabricate a laser emitting in terahertz frequency using the quantum-cascade structure. In 2002, the first THz QCL operating at 4.4 THz was demonstrated[10]. It is well known that terahertz technology has many potential applications, e.g., imaging, sensing, monitoring, communications, and so on. At present, the best records of device performance of terahertz QCLs are 1.2 THz for the lowest lasing frequency without the assistance of magnetic field[11], 117 K and 186 K for the highest CW and pulsed operating temperatures, respectively[12, 13], 248 mW for the highest output light power[14].

* Project supported by the Jiangsu University Initial Funding for Advanced Talents (No. 11JDG037).

† Corresponding author. Email: xfhe@ujs.edu.cn

Received 21 October 2011

2. Research progress terahertz semiconductor sources

2.1. n^+nn^+ $GaAs_{1-x}N_x$ THz diode

A strong negative differential velocity (NDV) effect in $GaAs_{1-x}N_x$ is observed when electrons are accelerated by an applied dc electric field into the NEM region of the subband. For an NDV system, any small fluctuation of internal inhomogeneity (doping or field) may result in a global current instability in realistic devices under certain conditions. The complex patterns of self-oscillating currents are the results of the formation and traveling of electric-field domains due to spatial amplification and temporal growth[15]. Detailed calculations[16] of current oscillations in n^+nn^+ $GaAs_{1-x}N_x$ diodes with an NEM n-base were carried out by using the transient drift–diffusion equations and the Poisson equation. The total current density is the sum of the conduction current density and the displacement current density.

When the applied voltage V_{dc} is larger than a critical value, self-sustained current oscillations appear. The current self-oscillations in doped n^+nn^+ diodes have been simulated by changing the electron concentration of the n-region and the applied DC electric field. Calculations indicate that the carrier concentration has a strong effect on the modes of electric field domains in n^+nn^+ diodes. The n^+nn^+ $GaAs_{1-x}N_x$ diode (the length of the n-base is 0.05 μm) exhibits undamped time-periodic current oscillations when the doping density N_d and the applied voltage are in proper region, as shown in Figs. 1(a) and 1(b).

In Fig. 1(a) we show the temporal evolution of the current $J(t)$ at a DC electric field $V_{dc} = 0.5$ V and different doping concentrations. In Fig. 1(b) the current oscillation is clearly shown. From Fig. 1(a), we can see that the current oscillation exists only when the doping density is in a particular region. Above or below the critical values it disappears. It can be concluded from Fig. 1 that when the applied dc electric field is fixed, the frequency of the current oscillation decreases as increasing the doping concentration and that at a fixed doping concentration, the frequency decreases as the applied DC electric field increases.

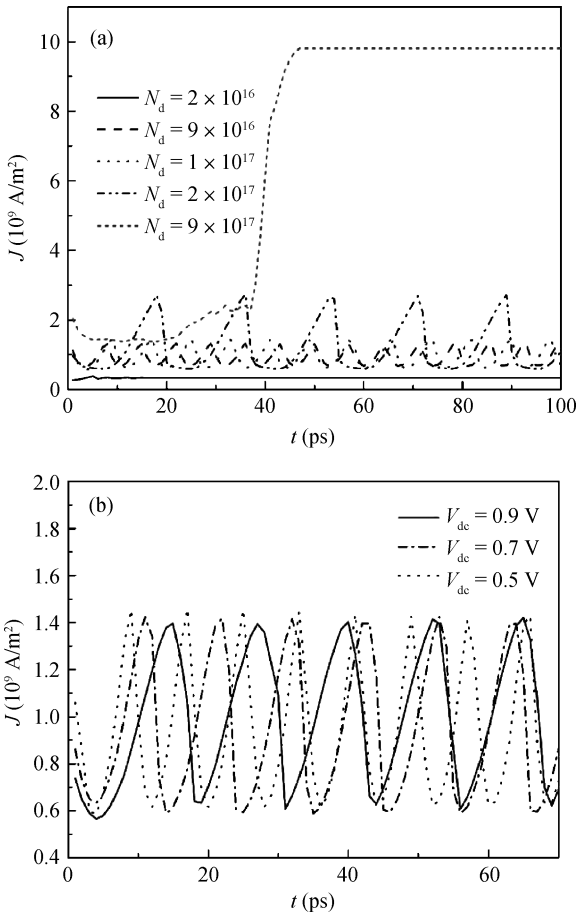

Fig. 1. (a) Temporal evolution of the current $J(t)$ at a DC electric field $V_{dc} = 0.5$ V and different doping concentrations. (b) Temporal evolution of the current $J(t)$[16].

2.2. Quantum-well NEM THz oscillator

The experiments in Refs. [7, 8] show that the dispersion relation for the ground subband of a p-type QW of zinc-blende-like semiconductors contains an extensive section with NEM due to the spin-orbit coupling of heavy- and light-hole states and the symmetry breaking of the QW potential. According to the nonparabolic balance-equation theory[9], Cao *et al.*[17] have calculated carrier drift velocity v_d as a function of steady-state electric field E in the x-direction at lattice temperatures $T = 77$ K, by accounting for the scatterings from the carrier impurity, the carrier-acoustic phonon (deformation and piezoelectric), the carrier-polar-optic phonon, and the carrier-nonpolar-optic phonon. The velocity-field curve for the NEM semiconductor has a N-shaped NDV. The NEM-induced NDV is the origin of the formation of the electric-field domain and current self-oscillation in the present NEM diodes. The calculated velocity-field relation is fed into the transient drift–diffusion model and the Poisson equation to study electric-field domain and self-oscillating characteristics of a DC-biased NEM p^+pp^+ diode. The total current density $J(t)$ is the sum of the conduction current density and the displacement current density. To mimic a realistic situation of the devices, a slight doping notch is assumed near the cathode end of the p^+pp^+ NEM diode. Here the p-base length of the NEM p^+pp^+ diodes is set to be $l = 0.3$ μm, and the doping concentration in the contact p^+-region is assumed to be 2×10^{18} cm^{-3}.

When a DC bias, V_{dc}, is applied to the NEM p^+pp^+ structure for a given doping concentration, N_a, there is a region of DC voltage band, in which dynamic electric-field domain is developed in the p-base and the self-oscillating current shows up with a frequency f_s. When the DC voltage is beyond the dynamic DC voltage band, only the static electric-field domain is formed, i.e., the current density approaches a constant after the initial transient dies out. To gain a clear insight into temporal evolution of current densities, current characteristics at lattice temperature $T = 77$ K are shown for the doping concentration $N_a = 7 \times 10^{16}$ cm^{-3}. In Fig. 2 we show the time-dependent current densities $J(t)$ in the dynamic DC voltage band as a density gray plot, where lighter areas correspond to larger current densities. The time delay is set to be from $t = 12$ to 19 ps for a clear view of the change in patterns. The patterns of the current densities are periodic with the time evolution, and

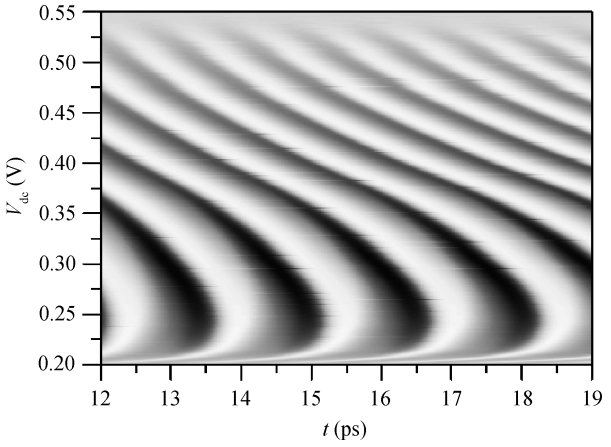

Fig. 2. Time-periodic self-oscillating current densities for the p^+pp^+ NEM diodes at $T = 77$ K and $N_a = 7 \times 10^{16}$ cm^{-3} are shown as a density gray plot, where lighter areas correspond to larger amplitudes of the current densities[17]. The corresponding oscillating frequencies lie in the THz range from 0.1 to 1.1 THz.

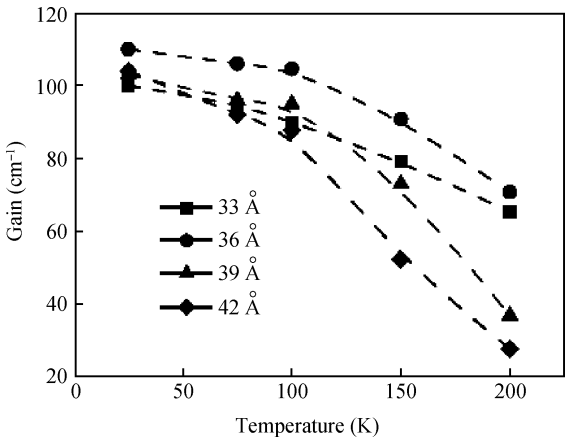

Fig. 3. Calculated gain for different extraction barrier widths as a function of temperature under corresponding injection anticrossing biases. The symbols represent sampling points and the dashed lines provide a guide for the eye[18].

the corresponding frequencies lie in the THz range from 0.1 to 1.1 THz.

2.3. MC simulation of THz QCL

The significant development of terahertz QCLs is attributed to the improvements of the active region design and the waveguide configuration. Since the first terahertz QCL, different approaches, i.e., chirped superlattices (CSL), the bound-to-continuum (BTC) transition and the resonant-phonon (RP) design, have been used to design active region structures. The first terahertz QCL[10] was based on a CSL structure in which the radiation transition is vertical, and the electron depopulation in the lower lasing state is achieved by the electron-electron scattering in minibands. The BTC design originates from mid infrared QCLs. Because of the diagonal transition, the BTC structure can largely reduce the threshold current density with the sacrifice of oscillation strength. Integrating the advantages of CSL and BTC designs, the RP design can make the radiation transition vertical and the depopulation of the lower lasing state efficient by using the rapid LO phonon scattering. One of the most powerful tools for investigating the carrier transport characteristics of THz QCLs is the MC method. In the MC model, we can intentionally turn on or off each scattering mechanism, i.e., electron–electron (ee), electron–phonon (ep), electron–impurity (ei) and the hot phonon effect, to investigate its influence on the transport properties of the device. The electron eigenstates and potentials which span three modules are obtained by solving the Schrödinger and Poisson equations, respectively. Li *et al.*[18] used the MC method to optimize the device parameters, i.e., injection barrier and extraction barrier widths, doping concentration, and phonon extraction level separation. It is found that the optimal extraction barrier for peak gain is 36 Å. To give a more applicable definition of the optimal barrier width, we also investigate the temperature performance of the structure with different extraction barrier widths. For all different extraction barrier widths, the calculated gains decrease with the increase of temperature as shown in Fig. 3. Compared to a structure with thicker extraction barriers (39 and 42 Å), the gain in the thinner barrier QC structure is found to degrade much more slowly with increasing temperature because of the slow reduction of population inversion. Our results give a qualitative analysis of the temperature performance and the trend is reasonably consistent with the experiments.

3. Summaries

In summary, THz semiconductor sources, such as $GaAs_{1-x}N_x$ Gunn-like diodes, quantum-well NEM THz oscillators, and THz QCLs, are reviewed. On the basis of the transient drift–diffusion model, steady-state electron transport and current oscillations in $GaAs_{1-x}N_x$ diodes and quantum-well the NEM THz oscillator are theoretically investigated, in which the current oscillations are the results of the formation and travel of electric field domains. By using the Monte Carlo method, the device parameters of resonant-phonon THz QCLs are optimized. The MC results are consistent with the experiments.

Acknowledgements

The author would like to thank Dr. H. Li for helpful discussions.

References

[1] Tisch U, Finkman E, Salzman J. The anomalous bandgap bowing in GaAsN. Appl Phys Lett, 2002, 81: 463
[2] Shan W, Yu K M, Walukiewicz W, et al. Band anticrossing in dilute nitrides. J Phys: Condens Matter, 2004, 16: S3355
[3] Ignatov A, Patan A, Makarovsky O, et al. Terahertz response of hot electrons in dilute nitride Ga(AsN) alloys. Appl Phys Lett, 2006, 88: 032107
[4] Cao J C, Lei X L. Hydrodynamic balance-equation analysis of spatiotemporal domains and negative differential conductance in a voltage-biased GaAs superlattice. Phys Rev B, 1999, 59: 2199
[5] Cao J C, Liu H C, Lei X L. Simulation of negative-effective-mass

terahertz oscillators. J Appl Phys, 2000, 87: 2867
[6] Cao J C. Interband impact ionization and nonlinear absorption of terahertz radiation in semiconductor heterostructures. Phys Rev Lett, 2003, 91: 237401
[7] Hayden R K, Maude D K, Eaves L, et al. Probing the hole dispersion curves of a quantum well using resonant magnetotunneling spectroscopy. Phys Rev Lett, 1991, 66: 1749
[8] Kash J A, Zachau M, Tischler M A, et al. Dispersion measurements of hot holes in quantum wells. Semicond Sci Technol, 1994, 9: 681
[9] Lei X L, Horing N J M, Cui H L. Theory of negative differential conductivity in a superlattice miniband. Phys Rev Lett, 1991, 66: 3277
[10] Köhler R, Tredicucci A, Beltram F, et al. Terahertz semiconductor-heterostructure laser. Nature (London), 2002, 417: 156
[11] Walther C, Fischer M, Scalari G, et al. Quantum cascade lasers operating from 1.2 to 1.6 THz. Appl Phys Lett, 2007, 91: 131122
[12] Williams B S, Kumar S, Hu Q, et al. Operation of terahertz quantum-cascade lasers at 164 K in pulsed mode and at 117 K in continuous-wave mode. Opt Express, 2005, 13: 3331
[13] Kumar S, Hu Q, Reno J L. 186 K operation of terahertz quantum-cascade lasers based on a diagonal design. Appl Phys Lett, 2009, 94: 131105
[14] Williams B S, Kumar S, Hu Q, et al. High-power terahertz quantum-cascade lasers. Electron Lett, 2006, 42: 89
[15] Cao J C, Li A Z, Lei X L, et al. Current self-oscillation and driving-frequency dependence of negative-effective-mass diodes. Appl Phys Lett, 2001, 79: 3524
[16] Feng W, Cao J C. Theoretical study of terahertz current oscillation in $GaAs_{1-x}N_x$. J Appl Phys, 2008, 104: 013111
[17] Cao J C. Current self-oscillations in negative effective mass terahertz oscillators. Chin Phys Lett, 2002, 19: 1519
[18] Li H, Cao J C, Lü J T, et al. Monte Carlo simulation of extraction barrier width effects on terahertz quantum cascade lasers. Appl Phys Lett, 2008, 92: 221105